One- and two-photon photoactivation of a paGFP-fusion protein in live *Drosophila* embryos

Janine N. Post*, Keith A. Lidke, Bernd Rieger, Donna J. Arndt-Jovin*

Department of Molecular Biology, Max-Planck-Institute for Biophysical Chemistry, Am Faßberg 11, 37077 Göttingen, Germany

Received 26 October 2004; revised 22 November 2004; accepted 23 November 2004

Available online 8 December 2004

Edited by Ulrike Kutay

Abstract **We constructed a photoactivatable *Drosophila* histone 2 A variant green fluorescent fusion protein (H2AvD-paGFP) for tracking chromatin loci in living *Drosophila* embryos. Activation of paGFP was achieved by irradiation from a single-photon diode laser at 408 nm, but activated nuclei failed to divide. Photoconversion could also be achieved by two-photon fs pulses in the range of 780–840 nm. Viability in whole-mount embryos could only be maintained at 820 nm, at which we could activate, simultaneously track and quantitate the mobility of multiple fluorescent loci. This report constitutes the first demonstration of two-photon activation of paGFP and the use of a paGFP-fusion protein in investigations of whole organisms.**

Keywords: Green fluorescent protein; Histone; Chromatin dynamics; Nuclear architecture; Two-photon microscopy; Photoactivation

1. Introduction

The cloning of the green fluorescent protein (GFP) visible fluorescent protein from *Aequorea victoria* in 1992 [1] and subsequent engineering of numerous variants [2] have revolutionized cell biological research. However, fluorescent labeling of an entire macromolecular assembly may obscure dynamic events such as transport or translocation. That is, there is a need for probes that can be selectively activated at a specific time and location. A photoactivatable GFP (paGFP) that fulfills this requirement was described recently [3]. Mutation of the threonine 203 to histidine in wild-type GFP (wtGFP) led to a decrease in the shoulder in the absorption spectrum at ~475 nm and a peak shift to 400 nm. Excitation at or near this wavelength leads to a photoconversion of the fluorophore, resulting in a 100-fold increase in the fluorescence above 500 nm using excitation at 488 nm. Since the background fluorescence from non-activated molecules is close to negligible, paGFP is an ideal candidate for the tracking of chimaeric proteins following activation by illumination restricted to a small volume element.

In the eukaryotic nucleus, the composition and organization of chromatin can have a profound effect on gene expression, such that gene insertion at different chromosomal locations may result in altered expression patterns and replication times [4]. The observation of chromatin dynamics in live cells requires specific labeling of chromosomes, for which few techniques are available [5–12], each of which has distinct limitations. The Lac operator (VFPLacI) system, introduced by Robinett et al. [12], has been exceptionally successful for observing chromatin movement and assessing protein-directed localization of DNA sequences, particularly in yeast [13]. However, in mammalian cells and *Drosophila*, only large arrays with large tandem repeats of DNA that show little or no movement have been studied to date [13–17]. Tandem sequence repeats may not reflect the behavior of native chromatin loci due to specific silencing mechanisms. Data from FISH in *Drosophila* that give a "snapshot in time" of the position of chromosomal loci previously demonstrated variations in locus position, implying large chromatin movements throughout the cell cycle [18]. In order to resolve the discrepancies between these two models of chromatin mobility we sought a method for marking the chromatin in vivo without disrupting the genomic structure.

The essential *Drosophila* histone variant, histone2AvD or H2AvD, offers several advantages over the core histones for viable methods for marking chromatin. The expression of the gene under its endogenous promoter is highly regulated and the fusion H2AvD-enhanced green fluorescent protein (eGFP) successfully rescues the lethal deficiency mutant [19] and serves as an excellent in vivo marker for chromatin [19]. We have determined by fluorescence recovery after photobleaching (FRAP) analysis that there is neither a significant pool of free H2AvD-eGFP nor an exchange of nucleosomal H2AvD-eGFP during non-S phase of the cell cycle (data of G. Ficz, not shown). Total marking of the chromatin with this protein, however, obscures high-resolution tracking of individual regions. Thus, we generated a transgenic fly-line expressing H2AvD-paGFP for marking, by photoactivation, multiple loci in single nuclei and single loci in multiple nuclei of whole mount living *Drosophila* embryos and imaginal discs. These spots were subsequently tracked in real-time by imaging using 488 nm excitation. paGFP has not been used previously in whole organisms. In this study, we characterize the activation of the fusion protein and the degree of cell viability after one- or two-photon activation.

*Corresponding authors. Fax: +49 551 2011467.
E-mail addresses: jpost@gwdg.de (J.N. Post); djovin@gwdg.de (D.J. Arndt-Jovin).

Abbreviations: eGFP, enhanced green fluorescent protein; paGFP, photoactivatable GFP; wtGFP, wild-type GFP; H2AvD, histone 2 A variant *Drosophila*; FRAP, fluorescence recovery after photobleaching; DIC, differential interference contrast; MSD, mean square displacement; SNR, signal-to-noise ratio; FWHM, full-width at half-maximum

0014-5793/$22.00
doi:10.1016/j.febslet.2004.11.092

2. Materials and methods

2.1. Generation of fly-lines

Drosophila melanogaster expressing H2AvD-eGFP were kindly provided by Dr. M. Clarkson [19]. H2AvD-paGFP was generated as follows: paGFP (a kind gift from Dr. J. Lippincott-Schwartz) was amplified by PCR using primers, 5′-GCCAGATCTATGGTG-AGCAAGGGCGAGG-3′ and 5′-CGGAGATCTCTTGTA-CAG-CTCGTCCATGCC-3′, and *Pfu* polymerase (Promega). The PCR products were cloned into PCRII using the TOPO TA-cloning strategy (version P, Invitrogen). paGFP was digested with *Bgl*II, treated with Klenow polymerase (New England Biolabs) and incubated with T4 DNA kinase (Roche). The DNA was ligated into the *Stu*I site of pc4B-histone2AvD (a kind gift of Dr. M. Clarkson). *D. melanogaster* expressing histone2AvD-paGFP were generated by injection of pc4B-H2AvD-paGFP-w^+ and p-helper into w^- embryos.

2.2. Sample preparation

Embryos were collected for 1–4 h on apple juice agar plates. After dechorionation the embryos were placed in a drop of Tyrode's buffer in a 2-well chamber slide (Nunc) and a 1–2 mm slice of apple juice agar was gently placed on top to prevent desiccation. Embryos remained viable for >4 h.

2.3. Microscopy and imaging

One-photon CLSM. The excitation beam of a 408 nm diode laser (Nichia, Japan) was coupled into a UV-Zeiss LSM310 yielding a power of 45 μW through the objective lens. An external shutter controlled the activation time (20–1000 ms). Images were acquired using 488 nm argon-ion laser excitation and emission >505 nm. The objective was a water immersion Zeiss C-ApoChromat 63× NA 1.2 W Korr.

Two-photon CLSM. A Tsunami Ti-Sapphire laser pumped by a Millenia solid-state laser (both Spectra Physics, Mountain View, CA) was coupled into the IR port of a Leica TCS SP2 microscope. The repetition rate was 82 MHz with 70 fs pulses [20]. The lateral full-width at half-maximum (FWHM) was 540 nm and the axial was 1800 nm. Images were acquired using argon ion laser excitation at 488 nm laser ($P = 8.5$ μW at the entrance to the objective) and an emission monochromator range of 505–680 nm. The objective was a water immersion Leica APO-CS 63× NA 1.2. Simultaneous differential interference contrast (DIC) images were also recorded. Due to the relatively low intensity of the photo-activated paGFP, we imaged using a pinhole opening of 12 airy units and did not acquire z sections to avoid photobleaching. We hope to have other microscopic equipment that can do fast, sensitive imaging in 3D in the near future.

2.4. Data and image analysis

For the image analysis we used specialized routines written in DIPimage [21]. The initial spot locations after activation were estimated after background subtraction (image before activation) and shading correction as follows: within a circular region of a few microns around the activation spots from the two-photon irradiation, bilateral filtering to reduce the noise, followed by a threshold was applied. The centers were computed and used as seeds for sub-pixel tracking by center-of-mass estimation. The mean square displacement (MSD) was computed over independent pairs as described in [22]. The tracks represent 2D projections in x–y of the 3D movement of each locus in the nuclear volume.

3. Results and discussion

3.1. One-photon microscopy: activation and nuclear viability

To investigate the chromatin organization and to visualize chromatin in distinct regions during cell division and development, we generated transgenic *D. melanogaster* lines expressing H2AvD-paGFP. We achieved activation of H2AvD-paGFP by excitation with a diffraction-limited spot from a 408 nm laser diode (Fig. 1) beginning with embryos at approximately stage 3. However, we observed that when

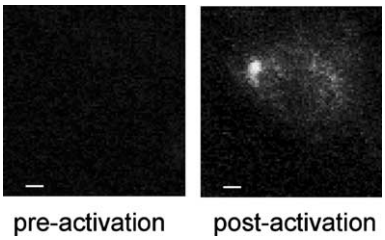

Fig. 1. Spot-photoactivation using a 408 nm diode laser. One locus in a live stage 5 embryo expressing H2AvD-paGFP was irradiated with a 408 nm diode laser for 1000 ms. Scale bar, 1 μm.

H2AvD-paGFP was activated in interphase nuclei under these conditions, the nuclei did not divide properly in subsequent cell cycles and were reabsorbed by the embryo. To investigate the cause of this photodamage, we performed similar irradiation protocols at 408 or 488 nm in embryos expressing non-activatable H2AvD-eGFP. The fate of irradiated nuclei was followed by the acquisition of confocal images at low intensity 488 nm excitation at 15 s intervals for 1 h. Fig. 2 shows nuclei in an early (stage 3) *Drosophila* embryo. Multiple nuclei were spot-irradiated with either 408 and 488 nm for 1000 ms (arrowheads) or only with 488 nm for 1000 ms (arrows, excitation powers were similar as in the nuclei irradiated at both wavelengths). Whereas the non-irradiated nuclei and the nuclei irradiated at 488 nm divided simultaneously, chromatin in nuclei irradiated at 408 nm failed to condense and were eventually re-absorbed by the embryo (45 min after irradiation).

In order to determine the source of toxicity we irradiated nuclei in embryos expressing a Polycomb-eGFP fusion protein that forms chromatin-associated protein complexes [23] and can be bleached to extinction by 488 nm excitation without organism toxicity (data of G. Ficz). We irradiated stage 5 embryos at 408 nm as above and observed a similar subsequent re-absorption of the irradiated nuclei as with H2AvD-eGFP or -paGFP (data not shown).

Irradiation of wild-type embryos, which did not express any GFP variant, was performed to determine whether absorption of 408 nm excitation by GFP or by other cellular constituents caused the phototoxicity. Again, the irradiated nuclei in these embryos failed to divide and were eventually re-absorbed by the embryo as could be seen using DIC (data not shown). These results indicate that the absorption of 408 nm light is mediated through other biomolecules rather than GFP to cause the photodamage. Interestingly, photoactivation using the 408 nm diode laser after formation of the metaphase plate did not inhibit division (Fig. 3, bottom panel). For comparison, a similar cell division in nuclei expressing H2AvD-eGFP is shown in the top panel of Fig. 3. We concluded that single photon 408 nm laser excitation at the intensity required for activation of paGFP was toxic to single nuclei/cells within the embryos and that normal chromatin dynamics and nuclear architecture may already be compromised immediately after irradiation and photoactivation. Although no information is available about the phototoxicity of the single photon activation of paGFP in mammalian cells in the literature, this problem should be addressed and the appropriate controls implemented to rule out toxicity or changes in physiology in other systems.

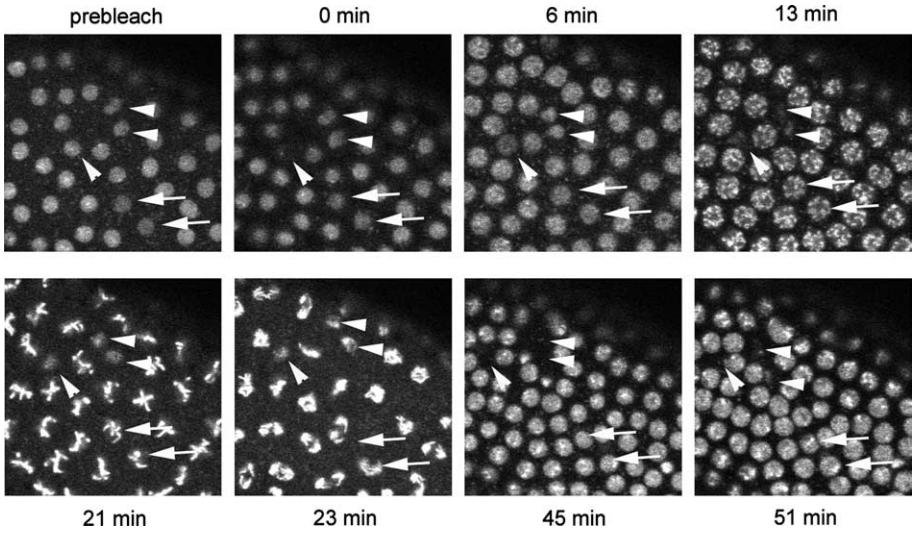

Fig. 2. Irradiation using 408 nm is toxic to individual nuclei. Individual nuclei of embryos expressing H2AvD-eGFP were irradiated at 408 nm (arrowheads). Nuclei were absorbed by the embryo within 50 min. Photobleaching using the 488 nm alone did not result in nuclear death (arrows).

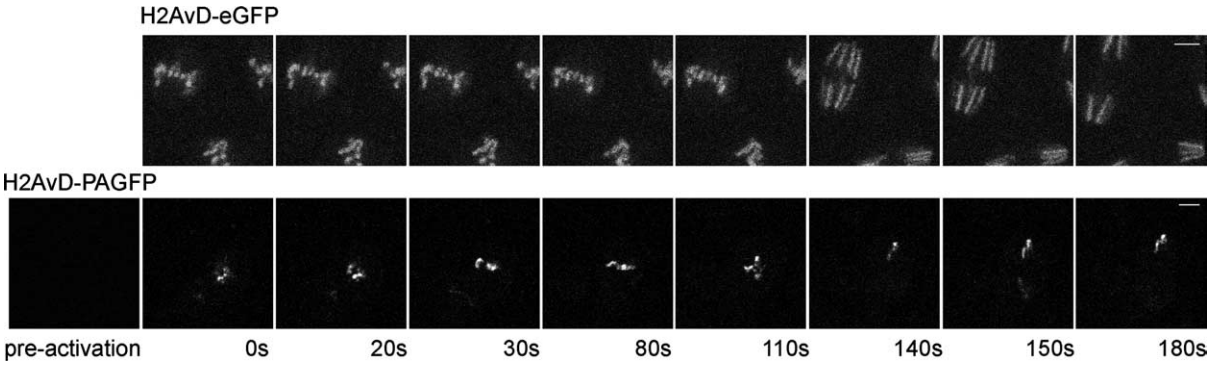

Fig. 3. Time-lapse of a dividing nucleus in a stage 5 *Drosophila* embryo. Top panel, nuclei from an embryo expressing His2AvD-eGFP. Bottom panel, nuclei from an embryo expressing His2AvD-paGFP, in which a part of the nucleus is photoactivated after formation of the metaphase plane. Scale bar, 5 μm.

3.2. Two-photon microscopy: activation and nuclear viability

Absorption of 408 nm light by the embryos may result in the generation of reactive oxygen species (ROS) known to be cytotoxic, causing damage to key cellular constituents such as proteins, lipids or nucleic acids [24,25]. Two-photon excitation reduces the volume element of the cell exposed to short wavelength exposure and can consequently reduce phototoxicity [26].

Two-photon excitation, whereby a fluorophore simultaneously absorbs 2 low-energy photons, is compatible with excitation of visible fluorescent proteins (VFPs), including wtGFP [26]. We tested activation of nuclei in stage 5 H2AvD-paGFP embryos at wavelengths between 780 and 840 nm in increments of 10 nm with subsequent imaging using 488 nm excitation. Successful activation occurred at wavelengths between 790 and 820 nm using a diffraction-limited spot. Powers above 1500 GW cm^{-2} yielded a signal-to-noise ratio (SNR) of up to 5-fold above background but resulted in non-viable nuclei. Similarly to the effect seen with single-photon activation, irradiation using two-photon at a wavelength of 820 nm at powers above 1500 GW cm^{-2} resulted in changes in chromatin morphology (Fig. 4). Different morphologies were dependent on the intensity of the two-photon laser and are indicative of chromosomal damage. We observed (i) abnormal chromatin condensation followed by absorption of the nuclei (Fig. 4A and B; 3200 GW cm^{-2}), (ii) non-disjunction of the nuclei, resulting in failure to divide and eventual reabsorption of the nuclei (Fig. 4C; 2600 GW cm^{-2}), and (iii) trailing metaphase chromosomes or bridges (Fig. 4D; 1700 GW cm^{-2}). Below 820 nm even powers of less than 1500 GW cm^{-2} were phototoxic. Table 1 summarizes these results. The optimum wavelength and excitation power that preserved viability of the nuclei over several cell divisions was determined to be 820 nm at 900–1500 GW cm^{-2} (Table 1). Under these conditions no difference was observed in the replication timing of irradiated vs. non-irradiated nuclei and we were able to track activated chromatin loci over several cell generations.

3.3. Real-time imaging of photoactivated loci

Even over very short time periods we observed rapid chromatin movement in stage 5 embryos, suggesting a behavior of the chromatin similar to that of yeast [16,17]. An example

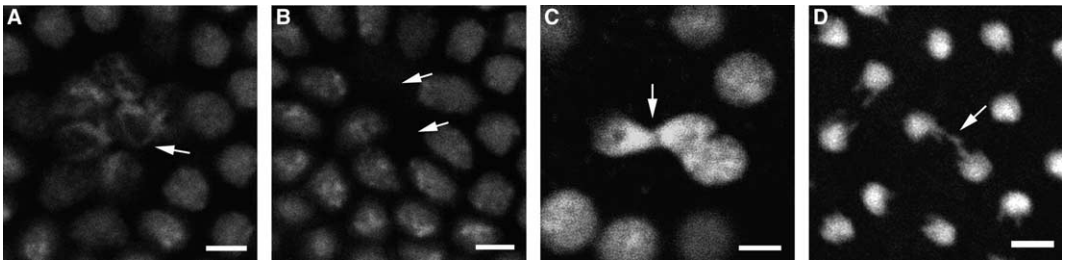

Fig. 4. Changes in chromatin morphology as observed after irradiation. Nuclei in embryos expressing His2AvD- eGFP were irradiated using two-photon irradiation at distinctive intensities. (A) Abnormal chromatin condensation followed by (B) absorption of the nuclei, 3200 GW cm^{-2}. (C) Non-disjunction of the nuclei, 2600 GW cm^{-2}. (D) Trailing metaphase chromosomes or bridges, 1700 GW cm^{-2}. Scale bar, 5 μm.

Table 1
Two-photon activation of paGFP-H2AvD: wavelength, power, and nuclear viability

Wavelength (nm)	Power (mW)[a]	Power density (GW cm^{-2})	Activation over background[b] (5 ms)	Nuclear viability	# Nuclear divisions
790	55	2300	2-fold	No	0
790	47.2	2000	<2-fold	No	0
790	28.3	1200	No	No	0
800	75	3200	2-fold	No	0
800	66	2800	<2-fold	No	0
800	40	1700	No	ND[c]	ND
810	75	3200	3-fold	No	0
810	66	2800	2-fold	No	0
810	40	1700	2-fold[d]	ND	ND
810	35	1500	2-fold[e]	ND	ND
810	5	210	No	Yes	>2
820	75	3200	10-fold	No	0
820	66	2800	3-fold	Reduced[f]	1
820	40	1700	2-fold	Reduced[g]	2 divisions
820	**35**	**1500**	**2-fold**[e]	**Yes**	**>2**
820	**22**	**940**	**2-fold**	**Yes**	**>2**
820	5	210	No	Yes	>2

[a]Through the objective.
[b]After 5 ms activation at the indicated power and wavelength.
[c]ND, not done.
[d]Activated spot bleaches within 100 images.
[e]Activated spot bleaches within 30 images.
[f]Nuclei die after division.
[g]Nuclei die after two divisions.

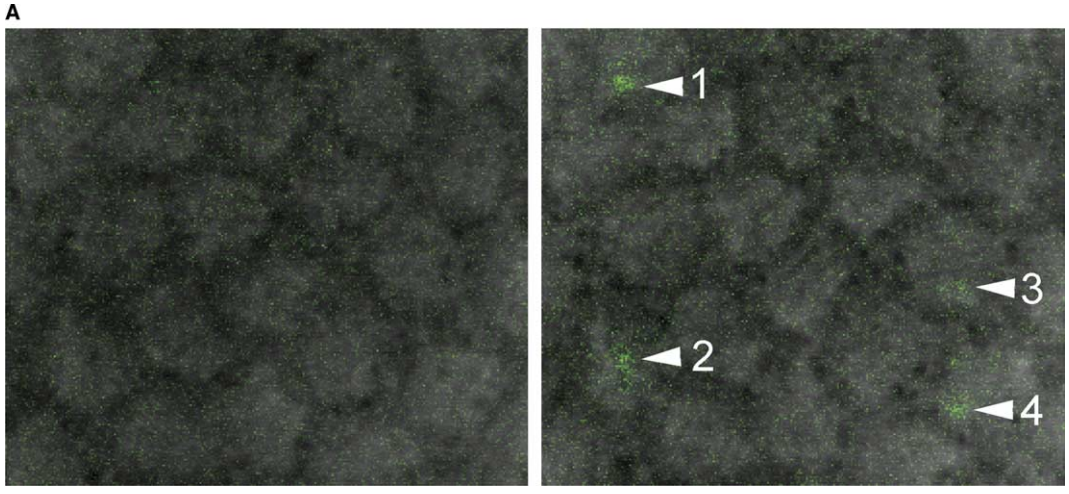

Fig. 5. Two-photon activation at 820 nm in a live stage 5 embryo, spot tracks and MSD plot of activated chromatin loci. (A) Pre-activation image using 488 nm excitation. Multiple loci were activated using two-photon activation at 820 nm and activated spots were imaged using a 488 nm laser. The fluorescent pre- and post-activation images are superimposed on simultaneous DIC images. Scale bar, 1 μm. (B) Individual tracks of photoactivated chromatin loci over 300 s. (C) The MSD plot shows restricted diffusion and not directed movement of the activated loci.

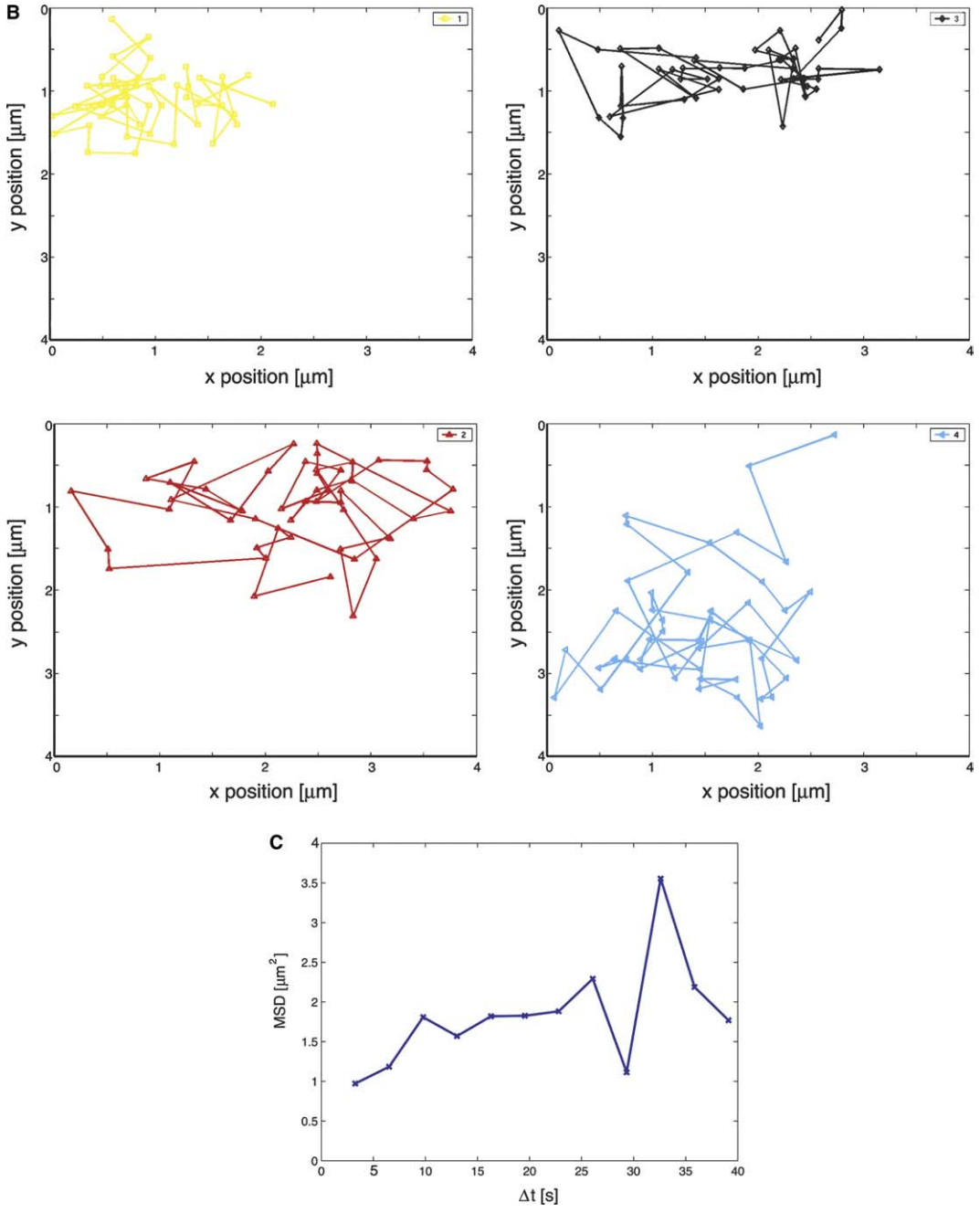

Fig. 5 (*continued*)

of this movement is shown in Fig. 5. Different loci in multiple nuclei of a stage 5 embryo were irradiated for 5 ms with a diffraction-limited spot at 820 nm (1500 GW cm^{-2}) and images were recorded every 2 s for 3 min using 488 nm excitation (8.5 μW). The relatively short activation times when using two-photon activation (5 ms vs. 1000 ms when using a 408 nm diode laser) allow for fast activation of multiple spots in the sample that can be tracked simultaneously. The tracks represent 2D projections in *x–y* of the 3D movement of each locus in the nuclear volume. For identification of the nuclear boundaries, simultaneous DIC images were recorded for each frame and were overlaid with the activated loci (Fig. 5). The activated loci, which ranged in size from 0.2 to 0.8 μm^2, were tracked using specialized routines written in DIPImage [21] and MSD plots for each locus were generated as described in Section 2.4. From the curve of the averaged MSD for these loci as shown in Fig. 5C, we conclude that all of the movements are subject to restricted diffusion. The average diffusion constant calculated from the initial slope of the MSD plots yields 2×10^{-2} $\mu m^2\,s^{-1}$, a value comparable to those found in yeast [15,16] and meiotic *Drosophila* nuclei [27] although the restricted area of ~1.3 μm is much larger than in those studies. A complete report of chromatin mobility measurements for various nuclear locations and for different stages of development will be presented elsewhere.

4. Conclusion

We have shown that paGFP can be photoactivated by diffraction limited two-photon pulsed laser excitation in live *Drosophila* embryos while maintaining viability of the organism. The optimal wavelength for both activation and cell viability is 820 nm at a maximum irradiance of 1500 GW cm^{-2}. We demonstrated that photoactivated loci can be tracked over time and the data used to calculate chromatin mobility.

Acknowledgments: The authors thank Dr. Cornelia Fritsch for help with the fly genetics and Drs. Cornelia Fritsch and Thomas M. Jovin for help in editing the manuscript. This project was supported in part by Grant #AR246-2-2 from the Deutsche Forschungs Gemeinschaft (DFG) to D.A.J. B.R. was supported by a TALENT fellowship of the Netherlands Organization for Scientific Research (NWO). We are grateful to Dr. Juergen Klingauf for use of the two-photon scanning microscope and to Edward Lemke for assisting us with the setup. We thank Dr. Michael Clarkson for the gift of a *Drosophila melanogaster* line expressing H2AvD-eGFP and the pc4B-H2AvD vector and Dr. Jennifer Lippincott-Schwartz for the paGFP vector.

References

[1] Prasher, D.C., Eckenrode, V.K., Ward, W.W., Prendergast, F.G. and Cormier, M.J. (1992) Primary structure of the *Aequorea victoria* green-fluorescent protein. Gene 111, 229–233.
[2] Miyawaki, A., Sawano, A. and Kogure, T. (2003) Lighting up cells: labelling proteins with fluorophores. Nat. Cell Biol., S1–S7.
[3] Patterson, G.H. and Lippincott-Schwartz, J. (2002) A photoactivatable GFP for selective photolabeling of proteins and cells. Science 297, 1873–1877.
[4] Cremer, T. and Cremer, C. (2001) Chromosome territories, nuclear architecture and gene regulation in mammalian cells. Nat. Rev. Gen. 2, 292–301.
[5] Zink, D. and Cremer, T. (1998) Cell nucleus – chromosome dynamics in nuclei of living cells. Curr. Biol. 8, R321–R324.
[6] Schermelleh, L., Solovei, I., Zink, D. and Cremer, T. (2001) Two-color fluorescence labeling of early and mid-to-late replicating chromatin in living cells. Chromosome Res. 9, 77–80.
[7] Kanda, T., Sullivan, K.F. and Wahl, G.M. (1998) Histone-GFP fusion protein enables sensitive analysis of chromosome dynamics in living mammalian cells. Curr. Biol. 8, 377–385.
[8] Tumbar, T., Sudlow, G. and Belmont, A.S. (1999) Large-scale chromatin unfolding and remodeling induced by VP16 acidic activation domain. J. Cell Biol. 145, 1341–1354.
[9] Edelmann, P., Bornfleth, H., Zink, D., Cremer, T. and Cremer, C. (2001) Morphology and dynamics of chromosome territories in living cells. Biochim. Biophys. Acta 1551, M29–M40.
[10] Zink, D., Cremer, T., Saffrich, R., Fischer, R., Trendelenburg, M.F., Ansorge, W. and Stelzer, E.H.K. (1998) Structure and dynamics of human interphase chromosome territories in vivo. Hum. Genet. 102, 241–251.
[11] Dietzel, S. and Belmont, A. (2001) Reproducible but dynamic positioning of DNA in chromosomes during mitosis. Nat. Cell Biol. 3, 767–770.
[12] Robinett, C.C., Straight, A., Li, G., Willhelm, C., Sudlow, G., Murray, A. and Belmont, A.S. (1996) In vivo localization of DNA sequences and visualization of large-scale chromatin organization using Lac operator/repressor recognition. J. Cell Biol. 135, 1685–1700.
[13] Gasser, S.M. (2002) Visualizing chromatin dynamics in interphase nuclei. Science 296, 1412–1416.
[14] Chubb, J.R., Boyle, S., Perry, P. and Bickmore, W.A. (2002) Chromatin motion is constrained by association with nuclear compartments in human cells. Curr. Biol. 12, 439–445.
[15] Vazquez, J., Belmont, A.S. and Sedat, J.W. (2002) The dynamics of homologous chromosome pairing during male *Drosophila meiosis*. Curr. Biol. 12, 1473–1483.
[16] Hediger, F., Neumann, F., Van Houwe, G., Dubrana, K. and Gasser, S.M. (2002) Live imaging of telomeres: yKu and SIr proteins define redundant telomere-anchoring pathways in yeast. Curr. Biol. 12, 2076–2089.
[17] Heun, P., Laroche, T., Shimada, K., Furrer, P. and Gasser, S.M. (2001) Chromosome dynamics in the yeast interphase nucleus. Science 294, 2181–2186.
[18] Gemkow, M.J., Verveer, P.J. and Arndt-Jovin, D.J. (1998) Homologous association of the Bithorax-Complex during embryogenesis: consequences for transvection in *Drosophila melanogaster*. Development 125, 4541–4552.
[19] Clarkson, M. and Saint, R. (1999) A His2AvDGFP fusion gene complements a lethal His2AvD mutant allele and provides an in vivo marker for *Drosophila* chromosome behavior. DNA Cell Biol. 18, 457–462.
[20] Tan, Y.P., Llano, I., Hopt, A., Wurriehausen, F. and Neher, E. (1999) Fast scanning and efficient photodetection in a simple two-photon microscope. J. Neurosci. Meth. 92, 123–135.
[21] Luengo Hendriks, C.L., Rieger, B., Ginkel, M.v., Kempen, G.M.P.v. and Vliet, L.J.v. (1999) Available from: <http://www.ph.tn.tudelft.nl/DIPlib>.
[22] Saxton, M.J. (1997) Single-particle tracking: the distribution of diffusion coefficients. Biophys. J. 72, 1744–1753.
[23] Buchenau, P., Hodgson, J., Strutt, H. and Arndt-Jovin, D.J. (1998) The distribution of polycomb-group proteins during cell division and development in *Drosophila* embryos: impact on models for silencing. J. Cell Biol. 141, 469–481.
[24] Halliwell, B. and Gutteridge, J.M.C. (1999) Free Radicals in Biology and Medicine, 3rd edn., p. 980, Oxford University Press.
[25] Dixit, R. and Cyr, R. (2003) Cell damage and reactive oxygen species production induced by fluorescence microscopy: effect on mitosis and guidelines for non-invasive fluorescence microscopy. Plant J. 36, 280–290.
[26] Zipfel, W.R., Williams, R.M. and Webb, W.W. (2003) Nonlinear magic: multiphoton microscopy in the biosciences. Nat. Biotechnol. 21, 1369–1377.
[27] Vazquez, J., Belmont, A.S. and Sedat, J.W. (2001) Multiple regimes of constrained chromosome motion are regulated in the interphase *Drosophila* nucleus. Curr. Biol. 11, 1227–1239.